Earth and Planetary Science Letters 309 (2011) 10–20

Contents lists available at ScienceDirect

Earth and Planetary Science Letters

journal homepage: www.elsevier.com/locate/epsl

A 4-Ma record of thermal evolution in the tropical western Pacific and its implications on climate change

Li Li [a,*], Qianyu Li [a,b,**], Jun Tian [a], Pinxian Wang [a], Hui Wang [a], Zhonghui Liu [c]

[a] State Key Laboratory of Marine Geology, Tongji University, Shanghai 200092, China
[b] School of Earth and Environmental Sciences, University of Adelaide, SA 5005, Australia
[c] Department of Earth Sciences, The University of Hong Kong, Hong Kong, China

ARTICLE INFO

Article history:
Received 29 November 2010
Received in revised form 5 April 2011
Accepted 14 April 2011
Available online 26 July 2011

Editor: P. DeMenocal

Keywords:
tropical western Pacific
alkenone-based temperature
Plio-Pleistocene thermal evolution
temperature gradient

ABSTRACT

Orbital resolution thermal histories over the last 4 Ma at ODP Site 1143 in the tropical western Pacific are reconstructed using alkenone paleothermometry. The temperature profile is characterized by a steady state of ~29 °C with fluctuations <1 °C before 2.7 Ma and by a strong oscillating state from 2.7 Ma, largely due to cooling by up to 4 °C from ~29 °C in interglacial to 26 °C in glacial intervals. This implies a relative warm and stable surface hydrography during the early and mid Pliocene in this region influenced by the warm pool before temperature decreases in responding to global cooling and the formation of the distinct glacial stages since the late Pliocene. Therefore, the smaller SST gradient between tropical eastern and western Pacific and between southern and northern South China Sea before the late Pliocene indicates a super sized Pliocene Pacific warm pool, while the larger SST gradient since then marks progressively intensification of the zonal Walker circulation and meridional Hadley circulation, representing the monsoon circulations in the region. The intensification of the Walker and Hadley circulations over the tropical Pacific may also have helped on the onset of glaciations and subsequent deglaciations during the late Pliocene and Pleistocene.

1. Introduction

Since the Pliocene, the earth climate system shifted from warm climate to the prevailing cooler climate of the Pleistocene with periodical waning and waxing of polar ice sheets (Lisiecki and Raymo, 2005). As a potential analog of future climate, the Pliocene is similar to the present in the global geography and carbon dioxide concentration (estimated at ~370 ppm), although its global temperature was about 3 °C higher than pre-industrial (Ravelo et al., 2004). Model simulation of the mid-Pliocene climate by the Pliocene Research Interpretations and Synoptic Mapping (PRISM) Group reproduced warmer conditions than today at middle latitudes and even as much as 10–20 °C warmer at high latitudes, but with little temperature difference in the tropics (Dowsett et al., 1992). At ~2.7 Ma, the earth's climate system entered a state with progressive intensification of glaciations, as marked by dramatic increase of ice rafting debris (IRD) at high latitude localities, and subsequently with regular glacial–interglacial oscillations after the mid-Pleistocene. Especially at mid-Pleistocene, the climate system shifted from high frequency-low amplitude oscillations dominated by the 41 ka period of Earth's obliquity to low frequency-high amplitude oscillations dominated by the 100 ka period of the orbital eccentricity characteristic of the Pleistocene glacial–interglacial cycles.

The tropical region acts as a source of heat and moisture poleward transport to the high-latitude regions in the modern climate system. Thus, the tropical ocean, especially the western equatorial Pacific, where one of the warmest regions in world oceans—the Western Pacific Warm Pool (WPWP) develops and becomes a critical component of the global climate system (Cane, 1998). A number of paleothermometric studies have generated continuous sea surface temperature (SST) records documenting the past climate transition from global warmth to ice ages over the Pliocene–Pleistocene in different tropical regions (Brierley et al., 2009; Cleaveland and Herbert, 2007; Dekens et al., 2007; Herbert et al., 2010; Jia et al., 2008; Karas et al., 2009; Lawrence et al., 2006; Wara et al., 2005). Some modeling studies even show that SST changes in the tropics may have played an important role in regulating global climate changes (Brierley and Fedorov, 2010; Webster, 1994).

To elucidate the tropics as a factor of past climate change, we need to quantify the magnitude and timing of SST changes in tropic regions. For the last glacial cycle, about 3 °C fluctuations in the western equatorial Pacific have been enumerated using new paleothermetric methods (Lea et al., 2000; Visser et al., 2003), reversing an early conclusion of little SST change (Thunell et al., 1994). Glacial–interglacial temperature oscillations by about 3 °C can be traced back at least to the last 1.7 Ma (de Garidel-Thoron et al., 2005; Medina-Elizalde and Lea, 2005), and deglacial warming in the tropical Pacific appears to precede the polar ice sheet decay (Lea et al., 2000; Visser et al., 2003). A long time scale study

* Corresponding author.
** Correspondence to: Q. Li, State Key Laboratory of Marine Geology, Tongji University, Shanghai 200092, China.
E-mail addresses: lilitju@tonji.edu.cn (L. Li), qli01@tongji.edu.cn (Q. Li).

0012-821X/$ – see front matter © 2011 Published by Elsevier B.V.
doi:10.1016/j.epsl.2011.04.016

by Wara et al. (2005) reveals a continual (or "permanent") El Niño state during the early–mid Pliocene before zonal SST gradient increased significantly across the equatorial Pacific.

Unlike the long term cooling trend observed in the eastern Pacific and eastern Atlantic upwelling regions (Brierley et al., 2009; Dekens et al., 2007; Etourneau et al., 2009; Lawrence et al., 2006; Marlow et al., 2000; Wara et al., 2005), however, no obvious long term cooling since the Pliocene has been found in the western Pacific warm pool (Wara et al., 2005), although the recent work by Herbert et al. (2010) indicate progressive cooling in glacials over the past 3.5 Ma in the tropical ocean. Therefore, high resolution stratigraphic records are needed to elucidate the detailed thermal history in this region and its relationship with global climate change. Here, we present a millennial SST record over the last 4 Ma from the southern South China Sea (SCS). As one of the largest marginal seas in the western Pacific, the South China Sea is characterized by higher sedimentation rates and a deeper CCD than in the open Pacific (Wang and Li, 2009). Well-preserved deep sea sediment sequences recovered during Ocean Drilling Program Leg 184 prove the SCS has better archives than the oceanic western Pacific for paleoenvironmental reconstructions in the region.

2. Materials and methods

Ocean Drilling Program (ODP) Site 1143 (9°21.72′N, 113°17.11′E; water depth 2772 m) lies in the southern part of the SCS. Close to the western margin of the modern WPWP, the site has annual average temperature of ~28 °C (Fig. 1). Increasing solar radiation during summer and strong southwestern summer monsoon both act on local hydrology by driving the warm water from the south flowing northward, resulting in the homogenization high SST in the SCS with only insignificant variations between 28.5 and 29.5 °C; while in winter, a latitudinal temperature gradient of ~2 °C exists between the southern part (28–29 °C) and the northern part (26–27 °C), largely due to the seasonally reversed eastern Asian Monsoon (Wang and Li, 2009).

A total of 1588 samples were taken at 10 cm intervals for analyses of unsaturated alkenones from the core depths of 0–165.42 mcd (meter composite depth) at ODP Site 1143. Alkenones, a suit of long chain (C_{35}–C_{39}) unsaturated ethyl and methyl ketones, are biosynthesized by a few species of haptophyte algae which live in the modern surface water, such as *Emiliania huxleyi* and *Gephyrocapsa oceanica*. Laboratory culture and field experiments demonstrate that the unsaturation of alkenones ($U^{k'}_{37}$) in these species is quantitatively related to their growing temperature and thus can be used to reconstruct paleo-SST (Prahl et al., 1988; Müller et al., 1998; see Supplementary material 1 for the factors on this paleothermometer). Many studies based on $U^{k'}_{37}$ have been recently published, especially from tropical regions (e.g., Herbert et al., 2010; McClymont and Rosell-Melé, 2006).

The average temporal resolution by samples is ~3 ka based on the orbitally tuned foraminifer $\delta^{18}O$ age model (Tian et al., 2002) (Fig. 2). Sample preparation and $U^{k'}_{37}$ based-SST measurement are briefly described below. About 5 g freeze-dried samples were extracted ultrasonically four times by dichloromethane/methanol (3:1, V/V), after adding an internal standard. The extracts were concentrated (3000 rpm, 5 min) and then saponified with 3 ml of 6% KOH/methanol overnight. Neutral components were recovered by extraction with *n*-hexane four times, then separated into alkanes and alcohols by silica gel column. Alkenones within the alcohol subfraction were analyzed by gas chromatography after derivitization by N, O-bis (trimethylsily)-trifluoroacetamide (BSTFA) at 70 °C for 2 h.

Gas chromatography (GC) measurement was performed on a Trace GC 2000 chromatography (Finnigan, Thermo Electron) equipped with HP-1 capillary column (50 m × 0.32 mm × 0.17 μm, J&W) and flame ionization detector. Both the injector and detector were set at 300 °C. Helium was used as the carrier gas with a flow rate of 1.2 ml/min by splitless injecting. The oven was kept initially at 60 °C for 1 min, then was programmed from 60 °C to 200 °C at 20 °C/min, followed by 5 °C/min to 270 °C, then 1.3 °C/min to 300 °C (maintained for 18 min), 5 °C/min to 310 °C (maintained for 5 min). The standard deviation for $U^{k'}_{37}$ method is 0.006, corresponding to a standard error <0.2 °C for SST estimation in this study.

Mass Spectrometer (MS) operation: EI ion source with temperature of 200 °C and emission electron energy of 70 ev, mass range of *m/z* 50–600, connecting temperature of 300 °C (Trace DSQ, Finnigan, Thermo). GC/MS and alkenone standards were also used for the retention time to confirm that quantification of alkenone peak areas are not compromised by co-eluting compounds.

In this study, SST was calculated using the global equation for the comparison ($U^{k'}_{37} = 0.033 \times SST + 0.044$, Müller et al., 1998). Spectral analyses were performed using the AnalySeries Program (Paillard et al., 1996). Cross Blackman–Tuckey spectrum of SST and benthic $\delta^{18}O$ was carried out on 40% of the series between 0 and 4 Ma using a Bartlett window with a band width of 0.06 and 0.0002, respectively. Gaussian filtering of the normalized SST, planktonic and benthic $\delta^{13}C$

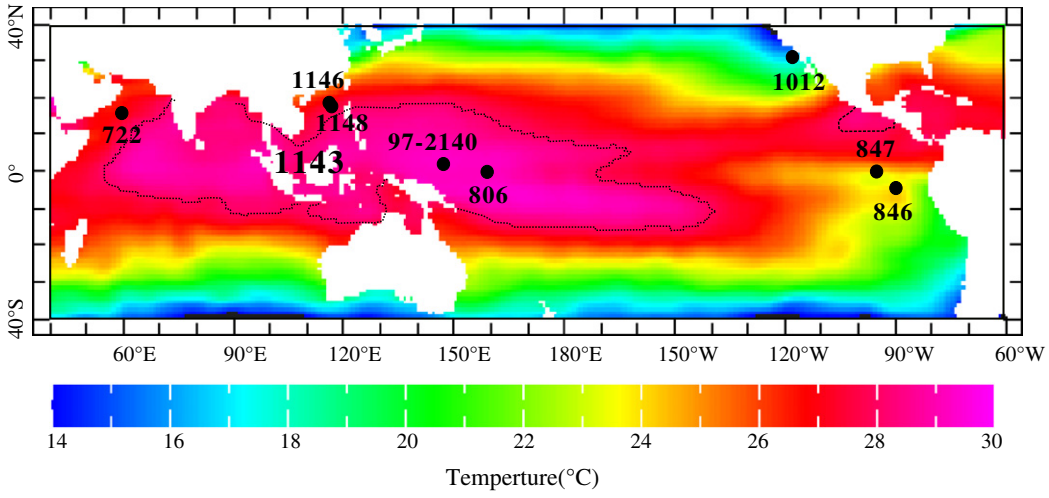

Fig. 1. Locations of ODP 1143 and other sites mentioned in the text. The modern mean annual sea surface temperature (SST) on the colored map was derived from: http://iridl.ldeo.columbia.edu/SOURCES/.LEVITUS94/.ANNUAL/.temp. The dashed line indicates the 28 °C isotherm.

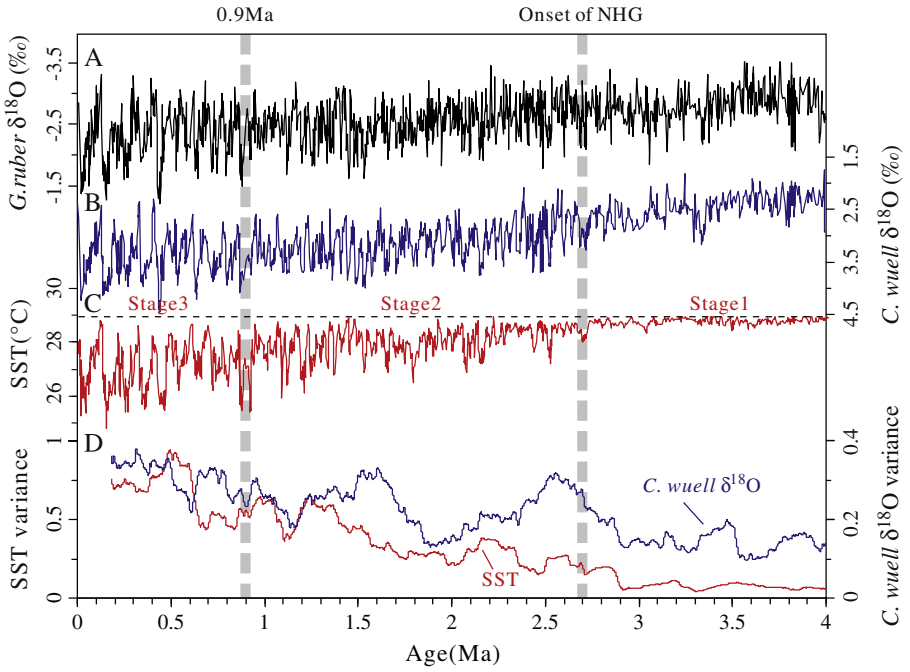

Fig. 2. Oxygen isotope and SST records over the last 4 Ma at ODP Site 1143, southern South China Sea. (A) planktonic foraminifer *Globigerinoides ruber* $\delta^{18}O$, (B) benthic foraminifer *Cibicidoides wuellerstorfi* $\delta^{18}O$ (Tian et al., 2002), (C) alkenone based SST, the dashed line correspond to the temperature of 28.97 °C that the $U^{k'}_{37}$ is equal to 1.0, (D) 200-ka moving windows of SST (red, left coordinate) and benthic $\delta^{18}O$ variability (blue, right coordinate). Vertical broad dashed lines mark major cooling events at 0.9 Ma (the mid-Pleistocene climate transition, or MPT) and at 2.7 Ma (the onset of northern hemisphere glaciation, or NHG).

was carried out at frequency 0.0025 ± 0.0005. All the analyses and measurements were undertaken in the State Key Laboratory of Marine Geology at Tongji University.

3. Results

Two kinds of C_{37} alkenones ($C_{37:2}$, $C_{37:3}$) were detected in the SCS sediment, although the proportion of $C_{37:3}$ alkenone was relatively low, even down to ~1 ng after 3 Ma. Overall, the measured $U^{k'}_{37}$ based-SST varied between 25 and 28.97 °C over the past 4 Ma, showing a trend very similar to the *Globigerinoides ruber* $\delta^{18}O$ record with small changes before the onset of northern hemisphere glaciations (NHG, ~2.7 Ma) and large changes thereafter, in addition to the obvious glacial–interglacial variations. From bottom to top, three stages can be identified (Fig. 2C, Supplementary material 2):

Stage 1 (4–2.7 Ma) features a high and stable temperature state. The average temperature is about 28.8 °C, with a fluctuation <0.5 °C, which approximates the standard error of the calibration. The signal of the $C_{37:3}$ alkenone is close to the instrument noise level, resulting in $U^{k'}_{37} \approx 1.0$ for some samples, which is close to the upper limit of the equation and corresponds to 28.97 °C(Fig. 2C). Higher temperature than these estimates is difficult to assess using the current method, but the absence of estimates <28 °C may imply that the record shown in Fig. 2C likely represents only the minimum SST variations for this interval at the studied site.

Stage 2 (2.7–0.9 Ma) shows a long term increasing temperature fluctuation trend, with the amplitude changing from 0.5 °C in the middle Pliocene to 3.2 °C in the middle Pleistocene. These changes are largely a consequence of intensified cooling during glacial intervals from 28.2 °C to 25.5 °C, or by about 1.4 °C/Ma; while the average interglacial SST remained stable at ~28.5 °C throughout this period.

Stage 3 (0.9 Ma–present) is characterized by up to ~3 °C glacial/interglacial temperature oscillations. Glacial SST averages at 26.2 °C with a range of 24.8 °C to 27 °C, and interglacial SST averages at 28.4 °C with a range of 27.8 °C to 28.8 °C (Fig. 2C).

4. Discussion

4.1. A reliable high resolution alkenone-SST record for the western tropical Pacific

Over the years, many studies have been devoted to SST variability and climate change in the western tropical Pacific (de Garidel-Thoron et al., 2005; Lea et al., 2000; McClymont and Rosell-Melé, 2006; Medina-Elizalde and Lea, 2005; Stott et al., 2002; Visser et al., 2003; Wara et al., 2005) (Table 1). Most of these studies are based on SST proxies of the Mg/Ca ratio in certain species but rarely on alkenones because the upper limit of the alkenone proxy approaches the annual average temperature in this region.

Fig. 3 compares SST records from three western tropical Pacific sites: the alkenone-based record at ODP 1143 and the Mg/Ca-based records at ODP 806 (Medina-Elizalde and Lea, 2005) and MD97-2140 (de Garidel-Thoron et al., 2005). The three curves show a similar thermal trend over the Pleistocene, with an average of about 29 °C in the interglacials and glacial–interglacial oscillations by 3–4 °C. Also at ODP 806, however, the alkenone-based study by McClymont and Rosell-Melé (2006) revealed slightly higher temperature values with relative weaker fluctuations than the Mg/Ca-based record. Over a longer interval, the $U^{k'}_{37}$-based SST for ODP 1143 also shows a trend similar to the relative lower resolution Mg/Ca-based SST for ODP 806 (Fig. 4A).

A comparable high-resolution study also based on alkenones has been recently published by Herbert et al. (2010) for ODP 1146 in the northern SCS but only for the last 2.1 Ma. The $U^{k'}_{37}$-based SST curves for ODP 1143 and ODP 1146 show a much better match except the consistently lower SST values by 2–4 °C from the latter site (Fig. 4A).

Table 1
Site location and data sources.

Site	Location	Water depth (m)	Method	Resolution (ka)	Interval (Ma)	References
West Pacific						
ODP1143	9° 21.72′ N, 113° 17.11′ E	2772	$U^{k'}_{37}$	2.5	0–4	This study
ODP1146	19° 27′ N, 116° 16′ E	2092	$U^{k'}_{37}$	1.6	0–2	Herbert et al. (2010)
ODP1148	18° 50.17′ N, 116° 33.94′ E	3294	$U^{k'}_{37}$	32	0–3.8	Jia et al. (2008)
MD97-2140	2° 2′ N, 141° 46′ E	2547	Mg/Ca	4.8	0–1.8	de Garidel-Thoron et al. (2005)
			$U^{k'}_{37}$	5	0.5–1.5	McClymont and Rosell-Melé (2006)
ODP 806	0° 19′ N, 159° 22′ E,	2520	Mg/Ca	2.4	0–1.4	Medina-Elizalde and Lea (2005)
				13.5	0–5.4	Wara et al. (2005)
East Pacific						
ODP1012	32° 17′ N, 118° 24′ W	1772	$U^{k'}_{37}$	2.0	0–4.1	Brierley et al. (2009)
ODP 847	1° 37′ N, 95° 48′ W,	2028	Mg/Ca	20	0–5.4	Wara et al. (2005)
ODP 846	3° 5′ S, 90° 49′ W	3296	$U^{k'}_{37}$	2.3	0–5.1	Lawrence et al. (2006)
ODP 849	0° 11′ N, 110° 31′ W	3839	$U^{k'}_{37}$	5	0.5–1.5	McClymont and Rosell-Melé (2006)
North Indian Ocean						
ODP 722	16° 37′ N, 59° 48′ E	2028	$U^{k'}_{37}$	2.0	0–3.3	Herbert et al. (2010)

ODP 1146 lies in the northern SCS, about 10° to the north of ODP 1143 (Fig. 1), so the two curves bearing similar features are not surprising.

However, discrepancies can still be noted between our high resolution $U^{k'}_{37}$-based SST record from the southern SCS and those SST records from the open western Pacific. At ~0.4 Ma, for example, SST at ODP 1143 is about 1.5 °C lower than the ODP 806 record. From 1.2 Ma to 0.95 Ma, SST at ODP 1143 is about 1–2 °C higher than the MD97-2140 record (Mg/Ca-based SST) (Fig. 3). SST fluctuation amplitudes for the Pliocene are also smaller (~0.5 °C) in our ODP 1143 record compared to other lower resolution records (1–2 °C) shown in Fig. 4A.

High SST of 30–32 °C before 3 Ma in the center of the WPWP has been proposed by adjusting the sea water Mg/Ca to the measured Mg/Ca values (Medina-Elizalde et al., 2008). Most of Mg/Ca-based SST reconstructions published recently were calculated using a constant seawater Mg/Ca parameter. According to Medina-Elizalde et al. (2008), however, the seawater Mg/Ca has changed over the last 5 Ma so significantly that SST calibrations using a constant parameter are not accurate and need adjustment. For SST estimates over period earlier than 1.6 Ma, for example, our $U^{k'}_{37}$-based SST for ODP 1143 from the SCS is ~1 °C higher than the original Mg/Ca-based SST for ODP 806 (Wara et al., 2005) from the center of the WPWP, indicating a bias toward lower SST values in the latter when ignoring seawater Mg/Ca adjustment. The adjusted Mg/Ca SST are 2–3 °C higher than the unadjusted SST for ODP 806 (Medina-Elizalde et al., 2008), or 1–2 °C higher than our $U^{k'}_{37}$-based SST for 1143 (Fig. 4A). A maximum SST at 30 °C or more for the region can be hypothesized on the feedback from the integration between warm water, evaporation/precipitation, atmospheric water vapor, cloud formation and associated albedo changes (Dowsett and Robinson, 2009).

Because of the limitation of the $U^{k'}_{37}$ method, the calibrated SST using Müller's equation will not go beyond 29 °C. However, the annual average SST in the central WPWP including ODP 806 locality is higher than 29 °C, which should be represented if methods used are not biased or self-constrained. High SST of 30–32 °C has been only rarely attained by using the Mg/Ca method but never by using the $U^{k'}_{37}$ method. Although a good match between the results of these two methods can be found from 0 to 1.4 Ma with strong fluctuations between different sites (Fig. 3), the calibrated SSTs for 1.4 Ma and older ages appear to fluctuate less strongly with maximum values rarely reaching 30 °C or more. Only after adjustments did the Mg/Ca-based SSTs for the 3–4 Ma interval at ODP 806 reach 30 °C and higher values (Medina-Elizalde et al., 2008), which are reasonable for the tropical western Pacific in the Pliocene when the seawater Mg/Ca was higher than today. The $U^{k'}_{37}$-based SST curve for ODP 1143 becomes flat at ~28.5 °C from ~2.8 Ma to older intervals, indicating a bias by the limitation of the method and/or partly by the site locality away from the WPWP center.

Generally, Mg/Ca-based SST estimates generate higher SST values, larger fluctuation amplitudes and higher frequency variability than the $U^{k'}_{37}$-based SST record due to higher sensitivity, higher analytical noise and/or higher inherent errors in the Mg/Ca-based SST method

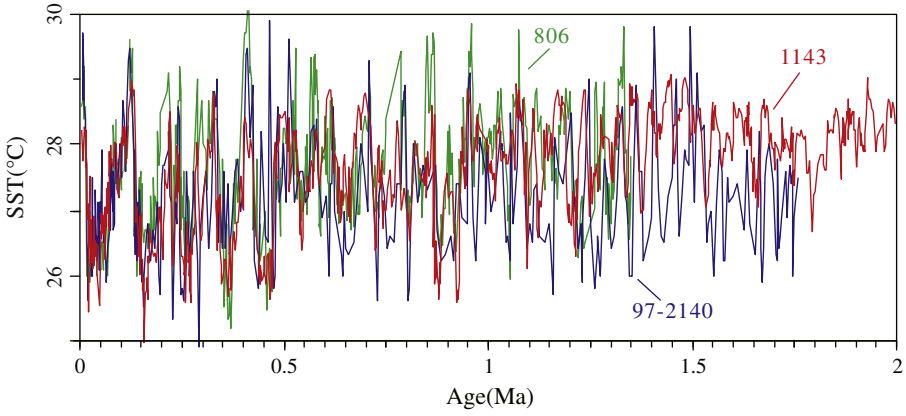

Fig. 3. Comparison between alkenone-derived SST record at ODP 1143 and Mg/Ca-derived SST records at ODP 806 (Medina-Elizalde and Lea, 2005) and from core MD97-2140 (de Garidel-Thoron et al., 2005) over the last 2 Ma.

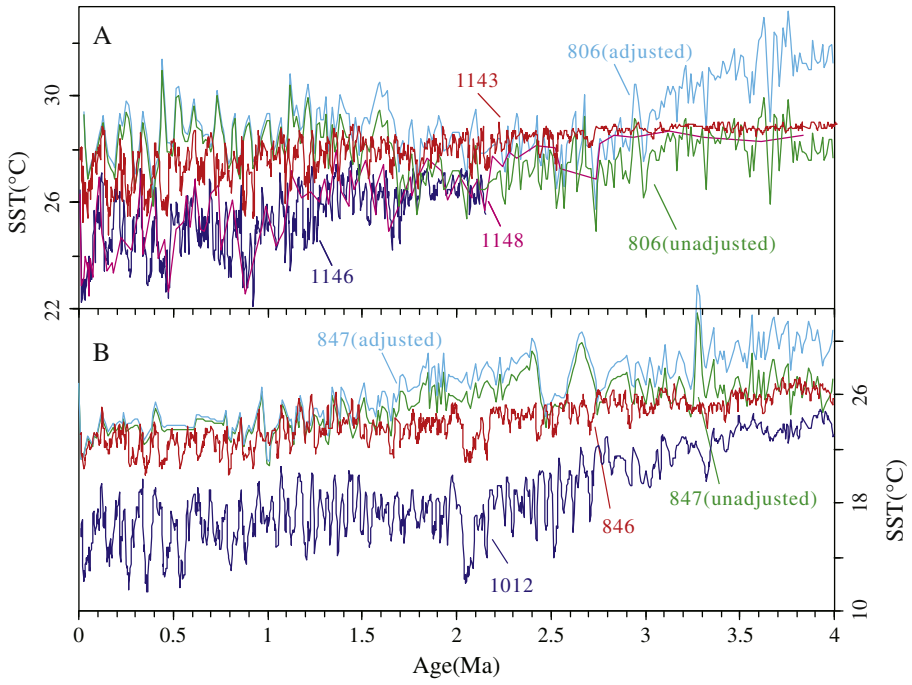

Fig. 4. (A) SST variations at ODP 1143 (red, this study), ODP 846 (blue, Lawrence et al., 2006), ODP 806 (green, unadjusted, Wara et al., 2005 and sky blue, adjusted, Medina-Elizalde et al., 2008), ODP 1146 (blue, Herbert et al., 2010) and 1148 (pink, Jia et al., 2008). (B) SST variations at ODP 846 (red, Lawrence et al., 2006), ODP 847 (green, unadjusted, Wara et al., 2005; sky blue, adjusted, Medina-Elizalde et al., 2008) and ODP1012 (Brierley et al., 2009).

(Dekens et al., 2008; Kiefer and Kienast, 2005). The differential bioturbational mixing of alkenones from coccolithphorides and foraminifera may be an alternative reason for the discrepancy from the alkenone method (Bard, 2001). Different ecological and physiological responses of the two organisms to environmental conditions other than temperature alone may be also an issue affecting the respective methods. Despite the different biases between the two geochemistry proxies and site locations, however, the overall similarity between these SST estimates confirms that the $U^{k'}_{37}$-based SST curve generated at ODP 1143 accurately reflects the sea surface temperature over the last for the southern SCS.

4.2. Major thermal stages in the Plio-Pleistocene tropical Pacific

4.2.1. The mid-Pliocene super western Pacific warm pool

The mid-Pliocene is characterized by warm SST all over the globe, with temperature values similar to today at low latitudes and significantly warmer than today at higher latitudes, particularly in the North Atlantic (Dowsett and Robinson, 2009; Dowsett et al., 1992). The mid-Pliocene warm period was originally defined as spanning 3.3–3 Ma by the PRISM Group, but high SST appears to extend for a much longer time and more obviously from the western Pacific. For example, the adjusted Mg/Ca-based SST higher than 29 °C at ODP 806 lasted from ~4 Ma to ~3.3 Ma (Fig. 4A, Medina-Elizalde et al., 2008), about 2 °C higher than the unadjusted record except for a few peaks (Wara et al., 2005). It is too early to confirm the adjustment method by Medina-Elizalde et al. (2008) be applicable to all regions, but unadjusted Mg/Ca-based SST records in the tropical Indo-Pacific are almost all slightly lower than the comparable $U^{k'}_{37}$-based SST records (Karas et al., 2009; Medina-Elizalde et al., 2008; Tian et al., 2005), suggesting a need for adjustment. Similarly, our SST record for the 4–2.7 Ma period at ODP 1143 is almost persistent at ~28.7 °C, which is similar to the modern value in the area. A constant 28.7 °C lasting for almost 2 Ma in the SCS may not have been realistic, but the static record likely sketches the general thermal trend with higher SST values omitted due to the limitation of the method itself. High and stable temperatures in the mid-Pliocene are also supported by fauna-based SST reconstructions by the PRISM group (Dowsett, 2007; Dowsett et al., 2005; Dowsett and Robinson, 2009).

Despite the absolute SST between the mid Pliocene and today is similar, temperature fluctuations are only ~0.5 °C in the mid Pliocene but up to 3–4 °C during glacial/interglacial transition in the late Pleistocene in the SCS (Fig. 2C). Across the tropical Pacific, glacial/interglacial temperature fluctuations range from 3 °C in the west to ~10 °C in the east, while the mid-Pliocene SST was 1–2 °C warmer than today in the west and 4–8 °C warmer in the east which is approaching 27 °C when upwelling was weak or absent(Fig. 4B) (Lawrence et al., 2006; Wara et al., 2005); longitudinally, the SST is approached to 28 °C in the mid Pliocene at ODP 1148 whose location is beyond the northern edge of the current warm pool, implying the longitudinal expansion of the WPWP (Fig. 4A; Jia et al., 2008). A temperature of ~26.5 °C on the northwestern site ODP 722 and ~24 °C on the far more northeastern site ODP 1012 during this time interval, both characteristically with slightly fluctuation, further corroborated the expanded WPWP (Brierley et al., 2009; Herbert et al., 2010). All these results reinforce a super sized warm pool during the mid-Pliocene.

4.2.2. Gradual glacial cooling during 2.7–0.9 Ma in the western tropical Pacific

The onset of glaciations at 2.7 Ma, which ended the mid-Pliocene warmth, has been documented by dramatic increases of ice rafting debris (IRD) in marine sediments at high latitudes (Haug and Tiedemann, 1998). It occurs as a sudden drop of ~1 °C in our SST estimates for ODP 1143 (Fig. 2C). As in Herbert et al. (2010), our record reveals that further temperature drops were gradual and occurred mainly during subsequent glacials, a feature missing from previous lower resolution records in the tropical Indian-western Pacific region (e.g., Karas et al., 2009; Wara et al., 2005) (Fig. 4A). The gradual cooling beginning from 2.7 Ma only during glacials is unique to the no upwelling tropical ocean, while cooling in most upwelling regions and high latitude regions occurred in both glacial and

interglacial periods sometimes dramatically (Brierley et al., 2009; Dekens et al., 2007; Etourneau et al., 2009; Herbert et al., 2010; Lawrence et al., 2006, 2009; Marlow et al., 2000; Wara et al., 2005).

Progressive glacial cooling in the tropical oceans recorded by the SST which fluctuated from 28.1–28.7 °C in 2.7 Ma to 25.4–28.7 °C in 0.9 Ma implied a stepwise global cooling trend, which is different from the relative regular oscillations between −3.1‰ and −1.9‰ throughout this time interval in the contemporary planktonic foraminifer $\delta^{18}O$ record (Fig. 2A, C). However, as early as 3.3 Ma, a major positive shift in benthic foraminifer $\delta^{18}O$ and a major drop in deep water temperature were observed, as well as a fast SST drop of ~2 °C in the tropical ocean records (Fig. 2B; Fig. 4A, B) (Brierley et al., 2009; Herbert et al., 2010; Lawrence et al., 2006; Sosdian and Rosenthal, 2009). As recorded by SST drop of 2 °C or more at many western Pacific localities, the major cooling event at 2.7 Ma appeared to have affected more than the 3.3 Ma cooling on the tropical warm pool. However, the signals of these two major cooling events in our record are relatively weak, especially the one at 3.3 Ma, probably due to the limitation of the method. The present method cannot detect temperature changes above 28.9 °C (using Müller's equation) due to alkenone with three unsaturated bonds which is absent in extremely warm environments. The upper temperature threshold may potentially underestimate temperature drop although the existence of a long-lasting warm SCS in the far western Pacific is not impossible when the passage between them remains wide and open during the mid and late Pliocene (Wang and Li, 2009).

Glacial cooling in the tropical region continued from 2.7 Ma to 0.9 Ma as marked by a low temperature of 25.5 °C. Since ~0.9 Ma, 41 ka asymmetric glacial–interglacial (G–IG) cycles developed with SST fluctuating between ~29 °C and 25.5 °C in the later part of the Pleistocene (Fig. 2, Fig. 7B and Section 4.4.1).

4.3. Zonal and meridional SST variations over the last 4 Ma

4.3.1. Zonal SST variations across the tropical Pacific

In the modern tropical Pacific, the westward trade winds drive upwelling of cooler waters in the east and pile up warmer waters in the WPWP, resulting in an east–west temperature gradient of 3 °C or more. This SST asymmetry across the tropic Pacific will be diminished by El Niño events due to a weakened Walker circulation. Changes in zonal SST gradients, therefore, provide the key evidence for the evolution of El Niño events and the Walker circulation strength (Lea et al., 2000; McClymont and Rosell-Melé, 2006; Wara et al., 2005). Although all these data resolution, including the following discussed data sets, are not appropriate for the discussion of the change of ENSO. Because higher eastern equator Pacific temperature and reduced east–west SST gradient only occur with the El Niño state in the modern normal ocean condition, we used the evidence of lower zonal temperature gradient during the mid-Pliocene to infer an El Niño-like state. For example, Wara et al. (2005) attribute the low zonal temperature gradient (~2 °C) between the western Pacific ODP 806 and eastern Pacific ODP 847 during the Pliocene warm period to "permanent" El Niño-like conditions, characterized probably also by substantially weaker interannual variability (Brierley et al., 2009).

To test these hypotheses, we compare the high resolution SST records between ODP 1143 in the far western Pacific and ODP 846 in the eastern Pacific, both based on alkenone paleothermometry. As shown in Fig. 5A, the mean temperature gradient ($\Delta SST_{1143-846}$) between the two sites increased from ~3 °C in the mid Pliocene to 5–6 °C in the late Pleistocene. These are similar to what has been reported by Wara et al. (2005) using Mg/Ca-based SST from ODP 806 and ODP 847, although the detailed gradient configurations between ODP 1143–ODP 846 and ODP 806–ODP 847 vary, likely relating to different analytic methods, different scales in sample resolution and different site locations. Increased zonal ΔSST since 4 Ma was mostly derived from larger SST drops at ODP 846 in the east, resulting in a similar trend between the absolute SST at this site and the $\Delta SST_{1143-846}$ (Fig. 5A). Similarly, sudden ΔSST increases were mainly caused by SST decreases in the east at sites ODP 846 and ODP 847, especially at 3.3, ~2.7, 2.4, 2.1, and 1.6 Ma. Noteworthy, however, is that some of these large ΔSST increases only occurred at one site rather than at both eastern sites, and further studies are needed to clarify their status and probable causing factors.

In principal, our data support the early finding that high SST with low fluctuations and the resultant lower zonal temperature gradient in the tropical Pacific during the early and mid Pliocene may have contributed to long lasting El Niño-like conditions (Wara et al., 2005; Dowsett and Robinson, 2009) and a super warm pool. However, ΔSST between the western and eastern Pacific increased gradually since the mid-Pliocene, implying progressive weakening in both the El Niño-like conditions and the super warm pool across the tropic Pacific (Fig. 5A). ΔSST increases by 2–6 °C continued until 1.6 Ma, occasionally with much larger jumps including the one at 2.1 Ma by 7.8 °C. Therefore, although weakening of the El Niño-like state and intensification of the Walker circulation began during the late Pliocene, a modern analog state started only from ~1.6 Ma, as revealed earlier from SST differences between the western and eastern tropical Pacific (Ravelo et al., 2004). At ~1.6 Ma, the thermocline in the tropical western Pacific also deepened as indicated by reduction in the deep dwelling benthic foraminifera (Chaisson and Ravelo, 2000; Jian et al., 2006). Apart from these, a series of other events occurred also at ~1.6 Ma, such as intensified upwelling off Namibia (Etourneau et al., 2009), increased algal productivity in the western equatorial Pacific (Lawrence et al., 2006) and obscuring of the long eccentricity signal in global $\delta^{13}C$ records (Wang et al., 2010), suggesting a large-scale change in global oceanography and climate.

During 1.6–0.9 Ma, the west–east ΔSST decreased mainly due to increasing SST during interglacial stages at ODP 846 in the east (Fig. 5A). The zonal ΔSST decreases may indicate a weakening Walker circulation, but whether the interglacial SST increases in the east were related to the return of an El Niño-like state is not clear. Since 0.9 Ma, after the dominant climate cycles shifted from 41 ka to 100 ka (Fig. 7B), the ΔSST between the western and eastern tropical Pacific has been fluctuating mainly between 3 and 6 °C, very similar to the modern normal value without an obvious El Niño or La Niña state (Fig. 5A). Fig. 6 shows a more simple sketch for periodical thermal evolution.

4.3.2. Meridional SST variations

Variations in meridional SST gradients between the southern and northern SCS are based on the orbital resolution records at ODP 1143 and ODP 1146 (Herbert et al., 2010) for the last 2 Ma and low resolution records at ODP 1143 (by smoothing) and ODP 1148 (Jia et al., 2008) for the last 4 Ma (Fig. 5B; Table 1). It is apparent from these records that the meridional thermal gradient from sites about 10° latitude apart in the SCS increased stepwise from ~1 °C in the Pliocene to ~5 °C at 0.9 Ma in the mid-Pleistocene before fluctuation mainly between 1 °C and 5 °C after 0.9 Ma. These meridional ΔSST changes in the SCS were consistent with the longitudinal ΔSST changes in the eastern Pacific by the low–mid latitude site comparison between the ODP 846 and ODP 1012, further confirming a weakening Hadley circulation both in west and east Pacific and a super-sized warm pool in the mid-Pliocene (Brierley et al., 2009; Jia et al., 2008), but a strengthening Hadley circulation and a somewhat contracted warm pool since the mid-Pliocene, respectively.

Due to the eastern Asian Monsoon, the modern SST varies between 28.5 and 29.5 °C for the whole SCS in summer and between 26 °C for the north and 28 °C for the south in winter (Wang and Li, 2009). The annual mean ΔSST between the northern and southern SCS is ~2 °C today, and ΔSST changes are closely related to winter monsoon strength (Tian et al., 2010). Therefore, the meridional ΔSST increases shown in Fig. 5B may also imply winter monsoon strengthening in the

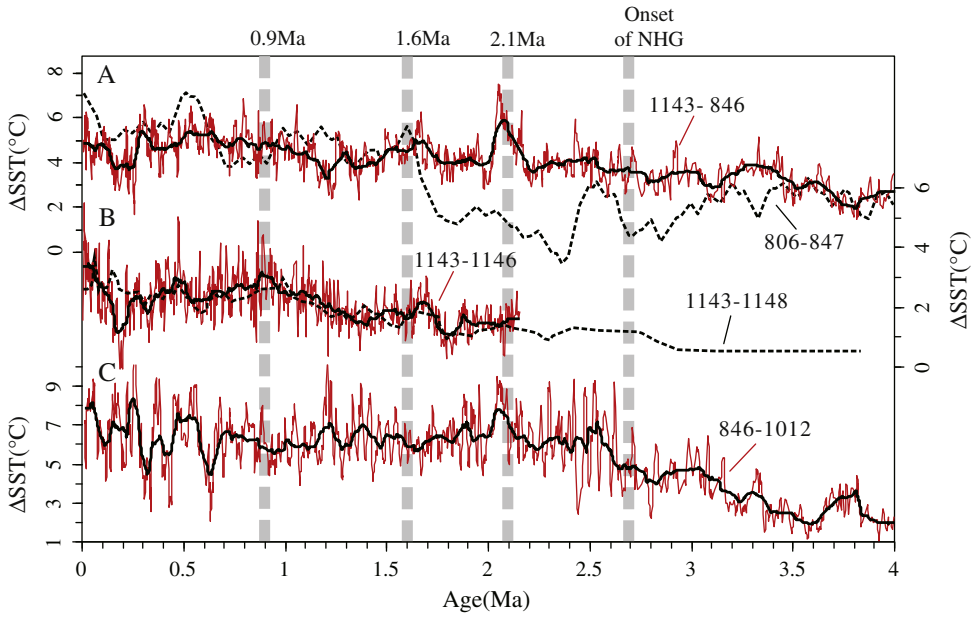

Fig. 5. (A) Zonal SST variations between tropical eastern and western Pacific: $\Delta SST_{1143-846}$ (red) and $\Delta SST_{806-847}$ (dashed line for the smoothing line, Wara et al., 2005), (B) meridional SST variations between northern and south SCS sites: $\Delta SST_{1143-1146}$ (red) and $\Delta SST_{1143-1148}$ (dashed smoothing line) (C) meridional SST variations between tropical and subtropical sites in the eastern Pacific: $\Delta SST_{846-1012}$ (Brierley et al., 2009). Vertical broad dashed lines mark major high temperature gradient events at 0.9 Ma, 1.6 Ma, 2.1 Ma and 2.7 Ma (or the onset of NHG). Black heavy lines in the millennial scale record denote the long-term trends.

SCS region since the Pliocene. Winter monsoon strengthening from the Pliocene to the Pleistocene was also recorded by increased deep dwelling fauna from ~40% to ~70% at ODP Site 1146 indicating a shoaling thermocline (Jian et al., 2006), by increased mass accumulation rate of eolian flux to the North Pacific (Rea et al., 1998) and by increased dust sedimentation rate on Chinese Loess Plateau (An et al., 2005). The progressive expansion of C4 plant and aridity in northeast Africa in this time interval appeared to have been caused also by a dry climate with strong winter monsoons (deMenocal, 2004; Feakins et al., 2005). Coupled ocean-atmosphere GCM3 numerical experiments by Brierley and Fedorov (2010) reinforce the importance of SST changes on the intensity of monsoons.

The meridional ΔSST increases in the SCS reached a maximal value of 5.2 °C at 0.9 Ma(Fig. 5B), the central point of the mid-Pleistocene climate transition, or MPT (Clark et al., 2006; Li et al., 2008; McClymont and Rosell-Melé, 2006). Large SST drops have been also recorded at many other tropical localities such as ODP 722, ODP 849 and ODP 846, coinciding with the coldest SST record in the tropical ocean (Herbert et al., 2010; McClymont and Rosell-Melé, 2006) and a large scale expansion of northern hemisphere ice sheets. Although the

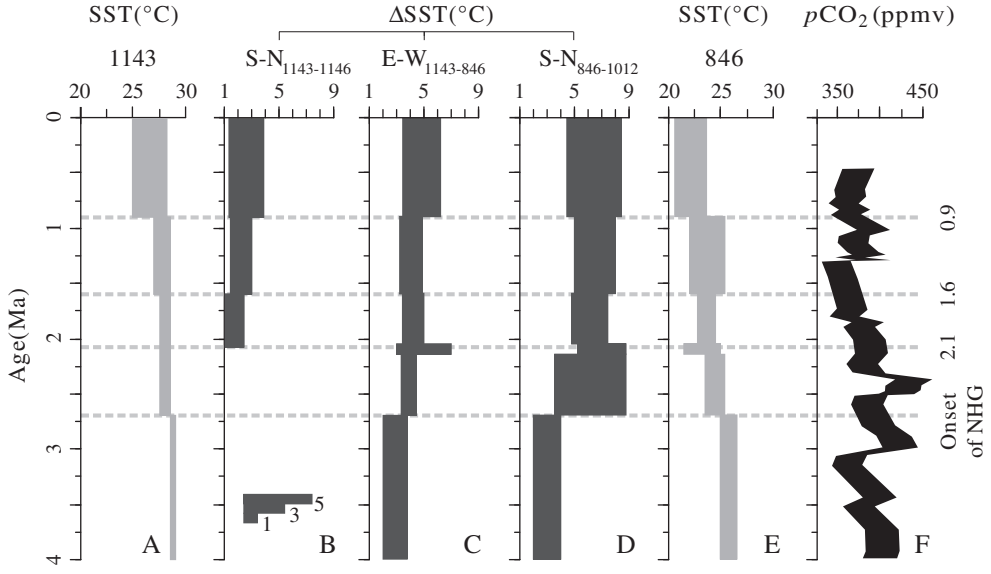

Fig. 6. Schematic illustration of SST evolution in ODP1143 (A), ODP846 (E), and their SST difference ($\Delta SST_{1143-846}$, C) and south–north SST difference in the western ($\Delta SST_{1143-1146}$, B) and eastern ($\Delta SST_{846-2012}$, D) Pacific. pCO_2 estimates at ODP 806,(Pagani et al., 2010). Level broad dashed lines mark major events at 0.9 Ma, 1.6 Ma, 2.1 Ma and 2.7 Ma, and the evolution was divided into several sections according to these boundary points. The width of each section indicates the average fluctuation range during the corresponding period. The extreme cooling in the eastern Pacific during 2–2.2 Ma is picked out as special period section in schematics which had a relationship with the eastern Pacific.

SST at ODP 806 and core MD97-2140 in the central of the warm pool on a long-term scale remained relatively stable (Fig. 3), a significant 0.9 Ma cooling at other sites indicates not only a considerable reduction in the size and strength of the warm pool but also more sensitive responses to global climate change from beyond its center. Although increased meridional temperature gradient alone may not directly trigger global glaciations (Brierley and Fedorov, 2010), it may have helped in reducing the polarward heat flux and enhancing high latitude cooling (de Garidel-Thoron et al., 2005).

In the eastern Pacific, the ΔSST between ODP 846 and ODP 1012 due to their far distance (~30° latitude) exhibits much larger fluctuations (Brierley et al., 2009) relative to the meridional ΔSST in the SCS (Fig. 5). Although direct comparison between these records for the interval of 4–2.1 Ma is not feasible because of a very low resolution of the $\Delta SST_{1143-1148}$ record, both the ΔSST curves feature an increasing trend from low in the mid Pliocene to high in the late Pliocene. This increasing trend terminated at ~2 Ma in the $\Delta SST_{846-1012}$ from the east but continued until ~0.9 Ma in the $\Delta SST_{1143-1146}$ and $\Delta SST_{1143-1148}$ from the west. Apart from this, however, ΔSST changes between these two regions appear to be largely in opposite directions particularly since 2.1 Ma, indicating different climate-oceanographic regimes with warm pool prevailing in the west and upwelling driven by high-latitude processes predominating in the east. However, strong oceanographic contrasts between the tropical western and eastern Pacific did not establish until ~1.6 Ma as discussed above.

4.4. Orbital forcing thermal evolution and carbon reservoir changes

4.4.1. Relationship between tropical SST and high latitude ice sheet growth

Relationship between tropical and high latitude climate changes during the Plio-Plistocene is not clear. Some studies reveal that the tropical SST leads the global ice volume change by ~2–3 ka yrs in the late Pleistocene (Lea et al., 2000; Medina-Elizalde and Lea, 2005; Visser et al., 2003), seemingly supporting a tropical forcing of the high latitude climate change. Other studies support a tightly coupled relationship of the tropical SST with global ice volume change and obliquity forcing, highlighting the impact of high latitude processes on tropical climate change (Herbert et al., 2010; Liu and Herbert, 2004).

The timing and amplitude variations of the SST at ODP 1143 and at other tropical sites indicate important influences from the onset of the NHG at ~2.7 Ma on the tropical SST change (Fig. 2). After ~2.7 Ma, the SST and benthic $\delta^{18}O$ exhibit nearly the same structure on both glacial–interglacial cycles and long-term changes. Gradual increases in the variance of the SST and benthic $\delta^{18}O$ records over the past 4 Ma also support tightly coupled relationship between the tropical SST and global ice volume change beginning from ~2.7 Ma (Fig. 2D). The two variance records show big discrepancy prior to ~2.7 Ma, but after 2.7 Ma the discrepancy gradually decreases and becomes small in the last 1 Ma. Increases in the amplitude of both SST and benthic $\delta^{18}O$ variances over the past 4 Ma demonstrate a shift of climate in high and low latitudes from a relatively stable state in the Pliocene and early Pleistocene to an unstable state since the mid Pleistocene. This shift is gradual in the global ice volume change as recorded by the gradual increase of the variance of the benthic $\delta^{18}O$, but relatively abrupt in the SST change as recorded by the fast increase of the variance of the SST after ~2.7 Ma relative to the stable variance before this time. If the pre-2.7 Ma SST record was not affected by the analytic limit, the early onset of the NHG at ~2.7 Ma could be viewed as a primary force pushing the tropical SST fluctuating away from its stable state before this time.

Response of the SST from the southern SCS to orbital forcing also amplifies after ~2.7 Ma. As recorded in the continuous wavelet analysis (CWT) (Fig. 7B), before ~2.7 Ma imprints of the astronomical forcing in the SST record are too weak to be recognized, but after ~2.7 Ma the orbital cycles including 400 ka, 100 ka, 41 ka and 23 ka abruptly become evident and particularly strong since the mid Pleistocene. The transition of the dominant cycle from 41 ka to 100 ka also occurs in the evolutive spectrums of the SST, exhibiting great resemblances to that of the benthic $\delta^{18}O$ (Berger et al., 1994). The 400 ka long eccentricity cycle in the SST record also becomes evident after ~2.7 Ma in the CWT (Fig. 7B). Tightly coupled relationship between the tropical SST and global ice volume after ~2.7 Ma can also be seen in the cross spectral analyses (Fig. 7A). Significant 19 ka, 23 ka, 41 ka and 100 ka cycles are found in the spectrum of the SST record over the past 4 Ma, and the SST record is coherent with the benthic $\delta^{18}O$ on the precession, obliquity and eccentricity bands. The almost near zero phase on the different primary orbital bands indicate that orbital cycles reflected by benthic $\delta^{18}O$ deducted ice volume change and the $U^{k'}_{37}$-based SST are in phase, although the SST contains a series of precession cycles ranging from 19 ka to 24 ka, rather than the distinct 19 and 23 ka peaks in the $\delta^{18}O$ record (Fig. 7A).

4.4.2. Relationship between tropical thermal evolution and carbon reservoir changes

Higher concentrations of atmospheric CO_2 has been proposed as the reason for the mid Pliocene warming by numerical experiments (Haywood et al., 2005). However, the estimated global CO_2 concentration of 365–415 ppm for the Pliocene (Fig. 6F, Pagani et al., 2010) is about 100 ppm higher than the preindustrial concentration and similar to the present value. As the present temperature is only 0.5 °C higher than the preindustrial, the 400 ppm CO_2 concentration alone cannot explain the global average warming of 3–4 °C in the mid-Pliocene. Besides CO_2, therefore, many other factors have been considered as contributing to the mid-Pliocene warm, including water vapor, another atmosphere's main greenhouse gas (Brierley et al., 2009), enhanced meridional ocean heat transport (Dowsett et al., 1992; Haywood et al., 2000) or large-scale planetary waves (Philander and Fedorov, 2003), frequent tropical cyclones (typhoons) through deep vertical mixing which affect the ocean's heat uptake and poleward heat transport (Fedorov et al., 2010), reduced ice sheet in both oceans and continents and reduced ice-albedo feedback (Haywood et al., 2005; Haywood and Valdes, 2004), or a combination of both the El Padre and Indian Ocean Dipole (Shukla et al., 2009). A recent study by Lunt et al. (2010) had shown that the global mean SST based on the p_{CO2} of 400 ppm and these short timescale physical factors will result in 1.6 °C increase, but after combining with some long timescale factors, i.e. topography, vegetation, and ice sheets, more than 1 °C extra higher temperature will be obtained. Moreover contemporary tectonic change, particularly the closure of the Indonesian seaway in the western Pacific and a shoaling Central American seaway in the eastern Pacific may also be considerable influence on the oceanographic feature which may be related with the given CO_2 forcing (Cane and Molnar, 2001; Haug and Tiedemann, 1998).

Just as warming was often associated with increased pCO_2, the major global cooling events at 2.7 and 0.9 Ma were respectively corresponding to periods with low or minimal pCO_2 (Fig. 6F) (Pagani et al., 2010; Tripati et al., 2009). Intensified chemical weathering and continental erosion due to further uplift of the Rocky Mountains and Himalayas (Raymo and Ruddiman, 1992; Ruddiman and Kutzbach, 1989) may have helped in reducing the global pCO_2 at these critical times of the Pliocene–Pleistocene. Apparently, few of so many hypotheses proposed to explain global warming and cooling have been widely accepted. Whether and how the global pCO_2 can be restored at subsequent interglacials also remain unclear. However, the SST in the tropical western Pacific would easily bounce back to 28 °C or more at each deglaciation and over all interglacial intervals as warm waters build up in the WPWP.

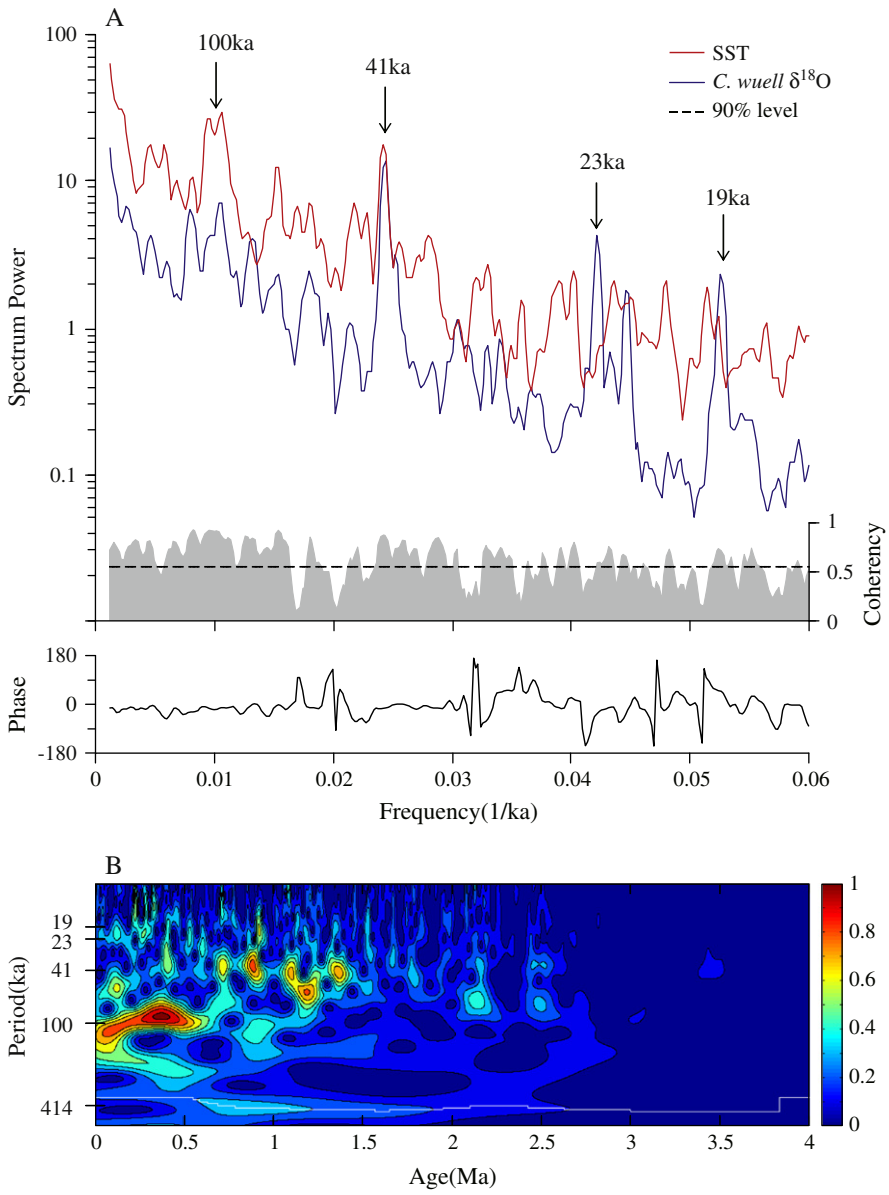

Fig. 7. (A) Cross Blackman–Tuckey spectrum of SST and benthic $\delta^{18}O$ at ODP1143 for the past 4 Ma using the AnalySeries software package (Paillard et al., 1996). Spectral densities are plotted on log scales. The horizontal dashed lines (red) indicate confidence at the 90% level in the coherence spectra. Periods of the main spectral peaks above the 90% confidence level are labeled. Positive phase denotes $-\delta^{18}O$ leading SST. (B) Evolution of spectral densities for the SST over the past 4.0 Ma by continuous wavelet analysis.

5. Conclusions

The alkenone-based SST record from ODP 1143 in the southern SCS provides insights into the thermal history of the western Pacific warm pool over the last 4 Ma. It confirms a super warm pool with El Niño-like conditions before 3 Ma and progressively intensified glaciations from ~3 Ma to 0.9 Ma before the development of typical glacial–interglacial cycles in the late Pleistocene. The relationship between tropical SST and polar ice sheet growth was weak before 2.7 Ma but strong after 2.7 Ma. Progressive SST decreases in the tropical western Pacific from 2.7 Ma to 0.9 Ma occurred mainly during glacial periods, while those in the east decreased during both glacial and interglacial periods, indicating enhanced warm pool effects on the west and upwelling effects on the east, especially after 1.6 Ma. SST variability at the tropical western Pacific enlarged and fluctuated mainly on 40 ka cycles from 2.7 to 0.9 Ma and then on 100 ka cycles after 0.9 Ma, responding to orbital forcing. The increases in both zonal and meridional thermal gradients since the mid-Pliocene also imply the intensification of the Walker circulation and Hadley circulation, or collectively the monsoon circulations in the region. These ΔSST increases across the low latitude Pacific preceding the onset of the NHG may signify the significant role played by tropical regions on the global climate changes. Beside the 2.7 Ma event which marks the NHG onset, other Plio-Pleistocene major cooling events at 1.6, and 0.9 Ma respectively all appear to have been corresponding with reduced pCO_2 implying the given CO_2 forcing.

Acknowledgments

This research used samples and data provided by the Ocean Drilling Program (ODP). ODP is sponsored by the US National Science Foundation (NSF) and participating countries under management of Joint Oceanographic Institutions (JOI), Inc. Funding for this research was provided by grants from the National Natural Science Foundation

of China (40976022, 40631007 and 41076017), the Ministry of Science and Technology of China (No. 2007CB815902 and No. 2007CB815904), and the China Geological Survey (Project H[2010] MA03-06-04). We thank Tim Herbert for discussions and comments on an early draft of the manuscript. Review and comments by Peter deMenocal and two anonymous reviewers significantly helped to improve the manuscript.

Appendix A. Supplementary data

Supplementary data to this article can be found online at doi:10.1016/j.epsl.2011.04.016.

References

An, Z.S., Huang, Y.S., Liu, W.G., Guo, Z.T., Clemens, S., Li, L., Prell, W., Ning, Y.F., Cai, Y.J., Zhou, W.J., Lin, B.H., Zhang, Q.L., Cao, Y.N., Qiang, X.K., Chang, H., Wu, Z.K., 2005. Multiple expansions of C-4 plant biomass in East Asia since 7 Ma coupled with strengthened monsoon circulation. Geology 33, 705–708.

Bard, E., 2001. Comparison of alkenone estimates with other paleotemperature proxies. Geochem. Geophys. Geosyst. 2, 1–12. doi:10.1029/2000GC000050.

Berger, W.H., Yasuda, M., Bickert, T., Wefer, G., Takayama, T., 1994. Quaternary time scale for the Ontong Java Plateau: Milankovitch template for Ocean Drilling Program Site 806. Geology 22, 463–467.

Brierley, C.M., Fedorov, A.V., 2010. Relative importance of meridional and zonal sea surface temperature gradients for the onset of the ice ages and Pliocene–Pleistocene climate evolution. Paleoceanography 25, PA2214. doi:10.1029/2009PA001809.

Brierley, C.M., Fedorov, A.V., Liu, Z.H., Herbert, T.D., Lawrence, K., LaRiviere, J.P., 2009. Greatly expanded tropical warm pool and weakened Hadley circulation in the early Pliocene. Science 323, 1714–1718. doi:10.1126/science.1167625.

Cane, M.A., 1998. Climate change — a role for the tropical Pacific. Science 282, 59–61.

Cane, M.A., Molnar, P., 2001. Closing of the Indonesian seaway as a precursor to east African aridification around 3 ± 4 million years ago. Nature 411, 157–162.

Chaisson, W., Ravelo, A.C., 2000. Pliocene development of the East-West hydrographic gradient in the Equatorial Pacific. Paleoceanography 15, 497–505.

Clark, P.U., Archer, D., Pollard, D., Blum, J.D., Rial, J.A., Brovkin, V., Mix, A.C., Pisias, N.G., Roy, M., 2006. The middle Pleistocene transition: characteristics, mechanisms, and implications for long-term changes in atmospheric pCO_2. Quatern. Sci. Rev. 25, 3150–3184.

Cleaveland, L.C., Herbert, T.D., 2007. Coherent obliquity band and heterogeneous precession band responses in early Pleistocene tropical sea surface temperatures. Paleoceanography 22, PA2216. doi:10.1029/2006PA001370.

de Garidel-Thoron, T., Rosenthal, Y., Bassinot, F., Beaufort, L., 2005. Stable sea surface temperatures in the western Pacific warm pool over the past 1.75 million years. Nature 433, 294–298.

Dekens, P.S., Ravelo, A.C., McCarthy, M.D., 2007. Warm upwelling regions in the Pliocene warm period. Paleoceanography 22. doi:10.1029/2006PA001394.

Dekens, P.S., Ravelo, A.C., McCarthy, M.D., Edwards, C.A., 2008. A 5 million year comparison of Mg/Ca and alkenone Paleothermometers. Geochem. Geophys. Geosyst. 9, 18.

deMenocal, P., 2004. African climate change and faunal evolution during the Pliocene–Pleistocene. Earth Planet. Sci. Lett. 220, 3–24. doi:10.1016/S0012-821X(04)00003-2.

Dowsett, H., Robinson, M.M., 2009. Mid-Pliocene equatorial Pacific sea surface temperature reconstruction: a multi-proxy Mid-Pliocene equatorial Pacific sea surface perspective. Philos. Trans. R. Soc. A 367, 109–125.

Dowsett, H., 2007. Faunal re-evaluation of Mid-Pliocene conditions in the western equatorial Pacific. Micropaleontology 53, 447–456.

Dowsett, H.J., Cronin, T.M., Poore, P.Z., Thompson, R.S., Whatley, R.C., Wood, A.M., 1992. Micropaleontological evidence for increased meridional heat-transport in the North Atlantic Ocean during the Pliocene. Science 258, 1133–1135.

Dowsett, H.J., Chandler, M.A., Cronin, T.M., Dwyer, G.S., 2005. Middle Pliocene sea surface temperature variability. Paleoceanography 20, PA2014. doi:10.1029/2005PA001133.

Etourneau, J., Martinez, P., Blanz, T., Schneider, R., 2009. Pliocene–Pleistocene variability of upwelling activity, productivity and nutrient cycling in the Benguela region. Geology 37, 871–874. doi:10.1130/G25733A.

Feakins, S.J., deMenocal, P.B., Eglinton, T.I., 2005. Biomarker records of late Neogene changes in northeast African vegetation. Geology 33, 977–980. doi:10.1130/G21814.1.

Fedorov, A.V., Brierley, C., Emanuel, K., 2010. Tropical cyclones and permanent El Niño in the early Pliocene. Nature 463, 1066–1070. doi:10.1038/nature08831.

Haug, G.H., Tiedemann, R., 1998. Effect of the formation of the Isthmus of Panama on Atlantic Ocean thermohaline circulation. Nature 393, 673–676. doi:10.1038/31447.

Haywood, A.M., Valdes, P.J., 2004. Modelling Middle Pliocene warmth: contribution of atmosphere, oceans and cryosphere. Earth Planet. Sci. Lett. 218, 363–377.

Haywood, A.M., Valdes, P.J., Sellwood, B.W., 2000. Global scale palaeoclimate reconstruction of the middle Pliocene climate using the UKMO GCM: initial results. Global Planet. Change 239–256.

Haywood, A.M., Dekens, P., Ravelo, A.C., Williams, M., 2005. Warmer tropics during the mid-Pliocene? Evidence from alkenone paleothermometry and a fully coupled ocean–atmosphere GCM. Geochem. Geophys. Geosyst. 6. doi:10.1029/2004GC000799.

Herbert, T.D., Peterson, L.C., Lawrence, K.T., Liu, Z.H., 2010. Tropical ocean temperatures over the past 3.5 million years. Science 328, 1530–1534.

Jia, G.D., Chen, F.J., Peng, P.A., 2008. Sea surface temperature differences between the western equatorial Pacific and northern South China Sea since the Pliocene and their paleoclimatic implications. Geophys. Res. Lett. 35, L18609. doi:10.1029/2008GL034792.

Jian, Z.M., Yu, Y.Q., Li, B.H., Wang, J.L., Zhang, X.H., Zhou, Z.Y., 2006. Phased evolution of the south–north hydrographic gradient in the South China Sea since the middle Miocene. Palaeogeogr. Palaeoclimatol. Palaeoecol. 230, 251–263.

Karas, C., Nürnberg, D., Gupta, A.K., Tiedemann, R., Mohan, K., Bickert, T., 2009. Mid-Pliocene climate change amplified by a switch in Indonesian subsurface throughflow. Nature Geosci. 2, 434–438.

Kiefer, T., Kienast, M., 2005. Patterns of deglacial warming in the Pacific Ocean: a review with emphasis on the time interval of Heinrich event 1. Quat. Sci. Rev. 24, 1063–1081.

Lawrence, K.T., Liu, Z.H., Herbert, T.D., 2006. Evolution of the eastern tropical Pacific through Plio-Pleistocene glaciation. Science 312, 79–83.

Lawrence, K.T., Herbert, T.D., Brown, C.M., Raymo, M.E., Haywood, A.M., 2009. High-amplitude variations in North Atlantic sea surface temperature during the early Pliocene warm period. Paleoceanography 24, PA2218. doi:10.1029/2008PA001669.

Lea, D.W., Pak, D.K., Spero, H.J., 2000. Climate impact of late Quaternary equatorial Pacific sea surface temperature variations. Science 289, 1719–1724.

Li, Q.Y., Wang, P.X., Zhao, Q.H., Tian, J., Cheng, X.R., Jian, Z.M., Zhong, G.F., Chen, M.H., 2008. Paleoceanography of the mid-Pleistocene South China Sea. Quat. Sci. Rev. 27, 1217–1233.

Lisiecki, L.E., Raymo, M.E., 2005. A Pliocene–Pleistocene stack of 57 globally distributed benthic $\delta^{18}O$ records. Paleoceanography 20, PA1003. doi:10.1029/2004PA001071.

Liu, Z.H., Herbert, T.D., 2004. High-latitude influence on the eastern equatorial Pacific climate in the early Pleistocene epoch. Nature 427, 720–723.

Lunt, D.J., Haywood, A.M., Schmidt, G.A., Salzmann, U., Valdes, P.J., Dowsett, H.J., 2010. Earth system sensitivity inferred from Pliocene modelling and data. Nature Geosci. 3, 60–64. doi:10.1038/NGEO706.

Marlow, J.R., Lange, C.B., Wefer, G., Rosell-Mele, A., 2000. Upwelling intensification as part of the Pliocene–Pleistocene climate transition. Science 290, 2288–2291.

McClymont, E.L., Rosell-Melé, A., 2006. Links between the onset of modern Walker circulation and the mid-Pleistocene climate transition. Geology 33, 389–392.

Medina-Elizalde, M., Lea, D.W., 2005. The Mid-Pleistocene transition in the tropical Pacific. Science 310, 1009–1012.

Medina-Elizalde, M., Lea, D.W., Fantle, M.S., 2008. Implications of seawater Mg/Ca variability for Plio-Pleistocene tropical climate reconstruction. Earth Planet. Sci. Lett. 269, 585–595.

Müller, P.J., Kirst, G., Ruhland, G., Storch, I.V., Rosell-Mele, A., 1998. Calibration of the Alkenone paleotemperature index U^{K}_{37} based on core-tops from the eastern South Atlantic and the global ocean (60° N–60° S). Geochim. Cosmochim. Acta 62, 1757–1772.

Pagani, M., Liu, Zh.H., LaRiviere, J., Ravelo, A.C., 2010. High Earth-system climate sensitivity determined from Pliocene carbon dioxide concentrations. Nature Geosci. 3, 27–30.

Paillard, D., Labeyrie, L., Yiou, P., 1996. Macintosh program performs time-series analysis. Eos Trans. AGU 77, 379.

Philander, S.G., Fedorov, A.V., 2003. Role of tropics in changing the response to Milankovich forcing some three million years ago. Paleoceanography 18. doi:10.1029/2002PA000837.

Prahl, F.G., Muehlhausen, L.A., Zahnle, D.L., 1988. Further evaluation of long-chain alkenones as indicators of paleoceanographic conditions. Geochim. Cosmochim. Acta 52, 2303–2310.

Ravelo, A.C., Andreasen, D.H., Lyle, M., Lyle, A.O., Wara, M.W., 2004. Regional climate shifts caused by gradual global cooling in the Pliocene epoch. Nature 429, 263–267.

Raymo, M.E., Ruddiman, W.F., 1992. Tectonic forcing of late Cenozoic climate. Nature 359, 117–122.

Rea, D.K., Snoeckx, H., Joseph, L.H., 1998. Late Cenozoic eolian deposition in the North Pacific: Asia drying, Tibetan uplift and cooling of the Northern Hemisphere. Paleoceanography 13, 215–224.

Ruddiman, W.F., Kutzbach, J.E., 1989. Forcing of Late Cenozoic Northern Hemisphere climate by plateau uplift in southern Asia and the American West. J. Geophys. Res. 94, 18409–18427.

Shukla, S.P., Chandler, M.A., Jonas, J., Sohl, L.E., Mankoff, K., Dowsett, H.J., 2009. Impact of a permanent El Niño (El Padre) and Indian Ocean Dipole in warm Pliocene climates. Paleoceanography 24, PA2221. doi:10.1029/2008PA001682.

Sosdian, S., Rosenthal, Y., 2009. Deep-sea temperature and ice volume changes across the Pliocene–Pleistocene climate transitions. Science 325, 306–310.

Stott, L., Poulsen, C., Lund, S., Thunell, R., 2002. Super ENSO and global climate oscillations at millennial time scales. Science 2002 (297), 222–226.

Thunell, R., Anderson, D., Gellar, D., Miao, Q., 1994. Sea surface temperature estimates for the tropical Western Pacific during the Last Glaciation and their implications for the Pacific warm pool. Quat. Res. 41, 255–264.

Tian, J., Wang, P.X., Chen, X.R., Li, Q.Y., 2002. Astronomically tuned Plio-Pleistocene benthic $\delta^{18}O$ records from South China Sea and Atlantic-Pacific comparison. Earth Planet. Sci. Lett. 203, 1015–1029.

Tian, J., Wang, P.X., Cheng, X.R., 2005. Quaternary upper ocean thermal gradient variations in the South China Sea: implications for east Asian monsoon climate. Paleoceanography 20, PA4007. doi:10.1029/2004PA001115.

Tian, J., Huang, E.Q., Pak, D.K., 2010. East Asian winter monsoon variability over the last glacial cycle: Insights from a latitudinal sea-surface temperature gradient across the South China Sea. Palaeogeogr. Palaeoclimatol. Palaeoecol. 292, 319–324.

Tripati, A.K., Roberts, C.D., Eagle, R.A., 2009. Coupling of CO_2 and ice sheet stability over major climate transitions of the last 20 million years. Science 326, 1394–1397.

Visser, K., Thunell, R.C., Stott, L., 2003. Magnitude and timing of temperature change in the Indo-Pacific warm pool during deglaciation. Nature 421, 152–155.
Wang, P.X., Li, Q.Y., 2009. The South China Sea: Paleoceanogrphy and Sedimentology. Springer. 506 pp.
Wang, P.X., Tian, J., Lourens, L.J., 2010. Obscuring of long eccentricity cyclicity in Pleistocene oceanic carbon isotope records. Earth Planet. Sci. Lett. 290, 319–330.
Wara, M.W., Ravelo, A.C., Delaney, M.L., 2005. Permanent El Niño-like conditions during the Pliocene warm period. Science 309, 758–761.
Webster, P.J., 1994. The role of hydrological processes in ocean–atmosphere interactions. Rev. Geophys. 32, 427–476.